

ORIGINAL
ARTICLE

Valproic acid attenuates blood–spinal cord barrier disruption by inhibiting matrix metalloprotease–9 activity and improves functional recovery after spinal cord injury

Jee Y. Lee,^{*,†} Hwang S. Kim,^{*,†} Hye Y. Choi,^{*} Tae H. Oh,^{*} Bong G. Ju[‡] and Tae Y. Yune^{*,†,§}^{*}Age-Related and Brain Diseases Research Center, Kyung Hee University, Seoul, Korea[†]Neurodegeneration Control Research Center, Kyung Hee University, Seoul, Korea[‡]Department of Life Science, Sogang University, Seoul, Korea[§]Department of Biochemistry and Molecular Biology, School of Medicine, Kyung Hee University, Seoul, Korea**Abstract**

The disruption of blood–spinal cord barrier (BSCB) after spinal cord injury (SCI) elicits an intensive local inflammation by the infiltration of blood cells such as neutrophils and macrophages, leading to cell death and permanent neurological disability. SCI activates matrix metalloprotease-9 (MMP-9), which is known to induce BSCB disruption. Here, we examined whether valproic acid (VPA), a histone deacetylase inhibitor, would attenuate BSCB disruption by inhibiting MMP-9 activity, leading to improvement of functional outcome after SCI. After moderate spinal cord contusion injury at T9, VPA (300 mg/kg) were immediately injected subcutaneously and further injected every 12 h for 5 days. Our data show that VPA inhibited MMP-9 activity after injury, and attenuated BSCB permeability and degradation of tight junction molecules such as occludin

and ZO-1. In addition, VPA reduced the expression of inflammatory mediators including tumor necrosis factor- α . Furthermore, VPA increased the levels of acetylated histone 3, pAkt, and heat-shock protein 27 and 70, which have anti-apoptotic functions after SCI. Finally, VPA inhibited apoptotic cell death and caspase 3 activation, reduced the lesion volume and improved functional recovery after injury. Thus, our results demonstrated that VPA improves functional recovery by attenuating BSCB disruption via inhibition of MMP-9 activity after SCI.

Keywords: blood–spinal cord barrier, histone deacetylase inhibitor, inflammation, matrix metalloprotease, spinal cord injury, tight junction.

J. Neurochem. (2012) **121**, 818–829.

The blood–brain barrier (BBB) including blood–spinal cord barrier (BSCB) is a highly specialized brain endothelial structure of the fully differentiated neurovascular system. When damaged by various insults including traumatic spinal cord injury (SCI), the BBB or BSCB disruption elicits blood infiltration and inflammation, thereby generating neurotoxic products that can compromise synaptic and neuronal functions (Hawkins and Davis 2005; Zlokovic 2005; Abbott *et al.* 2006) and induces the “programmed death” of neurons and glia, leading to permanent neurological deficits (Xu *et al.* 2001; Noble *et al.* 2002; Gerzanich *et al.* 2009).

Received November 29, 2011; revised manuscript received March, 8 2012, accepted March 9, 2012.

Address correspondence and reprint requests to Tae Young Yune, PhD, Department of Biochemistry and Molecular Biology, School of Medicine, Kyung Hee University, Medical Building 10th Floor, Dong-daemun-gu, Hoegi-dong 1, Seoul 130-701, Korea.

E-mail: tyune@khu.ac.kr

Abbreviations used: H3K9Ac, acetylated histone 3; BBB, blood–brain barrier; BSCB, blood–spinal cord barrier; COX-2, cyclo-oxygenase-2; GM, gray matter; HSP, heat-shock protein; HDAC, histone deacetylase; iNOS, inducible nitric oxide synthase; IL, interleukin; MBP, myelin basic protein; MMP, matrix metalloprotease; MPO, myeloperoxidase; PBS, phosphate-buffered saline; SCI, spinal cord injury; TNF- α , tumor necrosis factor α ; VPA, valproic acid; WM, white matter.

Matrix metalloproteases (MMPs), a family of zinc endopeptidases, are known to degrade extracellular matrix and other extracellular proteins (Sternlicht *et al.* 1999; Sternlicht and Werb 2001), and play roles in remodeling of the extracellular matrix, tissue morphogenesis, and wound healing (Werb and Chin 1998). However, excessive proteolytic activity of MMPs can be detrimental, leading to numerous pathological conditions including BBB or BSCB disruption after ischemic brain injury and SCI (Rosenberg *et al.* 1994, 1998; Rosenberg and Navratil 1997; Asahi *et al.* 2001; Xu *et al.* 2001; Noble *et al.* 2002) and inflammation (Mun-Bryce and Rosenberg 1998b). For example, MMP-9 induces proteolytic degradation of BBB and the white matter components, which results in an increase in infarct volume after transient cerebral ischemia (Asahi *et al.* 2001). MMP-9 also plays a key role in abnormal vascular permeability and inflammation in the early stages after SCI, and blocking of MMP-9 activity inhibits vascular permeability and improves functional recovery (Noble *et al.* 2002). These reports thus indicate that after SCI, an abnormal increase in MMP-9 in inflammatory cells or endothelial cells contributes to impairment of BSCB function by degrading the vascular basement membrane. Thus, we hypothesized that the inhibition of MMP-9 activity would stabilize the BSCB, inhibit inflammation and reduce cell death, thereby improve functional recovery after SCI.

Valproic acid (VPA), a short-chain fatty acid, is widely used for the treatment of seizures and bipolar mood disorder (Tunnicliff 1999; Johannessen 2000). VPA is well known to inhibit histone deacetylase (HDAC) at therapeutic levels (with an $IC_{50} = 0.4$ mM), causing histone hyperacetylation (Gottlicher *et al.* 2001; Phiel *et al.* 2001). HDAC is also implicated in the modulation of gene expression as well as life span in a variety of organisms such as yeast, *Caenorhabditis elegans* and *Drosophila* (Chang and Min 2002). Despite the precise mechanism underlying the therapeutic effects of VPA remaining elusive, a growing body of evidence shows that VPA is neuroprotective against a variety of insults *in vitro* and *in vivo*. For example, VPA prevents cortical neuronal cell death from ischemia (Kim *et al.* 2007; Qian *et al.* 2010) and protects spinal motor neurons in animal models of spinal muscular atrophy and amyotrophic lateral sclerosis (Feng *et al.* 1993; Tsai *et al.* 2008). VPA also exhibits neuroprotection in intracerebral hemorrhage and improves functional recovery after SCI by inhibiting histone deacetylase (Sinn *et al.* 2007; Lv *et al.* 2011). Furthermore, a recent report (Wang *et al.* 2011) shows that VPA reduces BBB disruption by inhibiting MMP-9 in a rat model of transient focal cerebral ischemia. Here, we tested the hypothesis that after SCI, VPA treatment would attenuate BSCB disruption by inhibiting MMP-9 activity and reduce apoptotic cell death thereby improve functional recovery.

Materials and methods

Spinal cord injury

Adult rats [Sprague–Dawley; male; 250–300 g; Sam:TacN (SD) BR, Samtako, Osan, Korea] were anesthetized with chloral hydrate (500 mg/kg) and a laminectomy was performed at the T9–T10 level exposing the cord beneath without disrupting the dura. The spinous processes of T8 and T11 were then clamped to stabilize the spine, and the exposed dorsal surface of the cord was subjected to moderate contusion injury (25 gm-cm) or moderately severe injury (50 gm-cm) using a New York University impactor as previously described (Lee *et al.* 2010). For the sham-operated controls, the animals underwent a T10 laminectomy without weight-drop injury. All surgical interventions and post-operative animal care were performed in accordance with the Guidelines and Policies for Rodent Survival Surgery provided by the Animal Care Committee of the Kyung Hee University.

Valproic acid administration

Valproic acid sodium salt (VPA) (Sigma, St Louis, MO, USA) was dissolved in sterile phosphate-buffered saline (PBS) and injected subcutaneously into animals. Rats were given VPA (150, 300 mg/kg) immediately after SCI and then were injected with a same dose of VPA every 12 h for 5 days. For the sham-operated controls, the animals underwent a T9–T10 laminectomy without contusion injury, and received no pharmacological treatment. Control (vehicle) groups received equivolumetric injection of PBS at the corresponding time points after injury. Significant side effects resulting from VPA treatment such as changes in body weight or an increase in mortality were not observed throughout experiments.

Gelatin zymography

The activity of MMP-2 and -9 at 1 day after injury was examined by gelatin zymography based on a previously described protocol with some modifications (Noble *et al.* 2002). Briefly, segments of the spinal cord containing the lesion epicenter or matched regions of the sham controls were dissected and frozen at -80°C . Each sample was weighed and homogenized in lysis buffer containing the following: 28 mM Tris–HCl, 22 mM Tris-base, pH 8.0, 150 mM NaCl, 1% Nonidet P-40, 0.5% sodium deoxycholate, and 0.1% sodium dodecyl sulphate. The protein concentration of the homogenates was determined by the bicinchoninic acid method (BCA protein assay kit, Pierce, Rockford, IL, USA). After determination of protein concentration of the homogenates, equal amounts of protein (30 μg) were loaded on a Novex 10% zymogram gel (EC61752; Invitrogen, Carlsbad, CA, USA) and separated by electrophoresis with 100 V (19 mA) at 4°C for 6 h. The gel was then incubated with renaturing buffer (2.5% Triton X-100) at 15 – 30°C for 30 min to restore the gelatinolytic activity of the proteins. After incubation with developing buffer (50 mM Tris–HCl, pH 8.5, 0.2 M NaCl, 5 mM CaCl_2 , 0.02% Brij35) at 37°C for 24 h, the gel was stained with 0.5% Coomassie blue for 60 min and then destained with 40% methanol containing 10% acetic acid until appropriate color contrast was achieved. Clear bands on the zymogram were indicative of gelatinase activity. Relative intensity of zymography (relative to sham or vehicle) was measured and analyzed by AlphaImager software (Alpha Innotech Corporation, San Leandro, CA, USA). Background was subtracted from the optical density measurements. Experiments

were repeated three times and the values obtained for the relative intensity were subjected to statistical analysis.

Tissue preparation

At specific time points after SCI, animals were anesthetized with chloral hydrate (500 mg/kg) and perfused via cardiac puncture initially with 0.1 M PBS and subsequently with 4% paraformaldehyde in 0.1 M PBS. A 20-mm section of the spinal cord, centered at the lesion site, was dissected out, post-fixed by immersion in the same fixative for 5 h and placed in 30% sucrose in 0.1 M PBS. The segment was embedded in optimal cutting temperature for frozen sections, and longitudinal or transverse sections were then cut at 10 or 20 μm on a cryostat (CM1850; Leica, Germany).

Measurement of blood–spinal cord barrier disruption

The integrity of the BSCB was examined with Evans blue dye extravasation according to previous reports (Chen *et al.* 2008; Tian *et al.* 2009) with minor modifications. At 1 or 5 days after SCI, 5 mL of 2% Evans blue dye (Sigma) solution in saline was administered intraperitoneally. Three hours later, animals were anesthetized and killed by intra-cardiac perfusion with saline. The T9 spinal cord segment was removed and homogenized in a 50% trichloroacetic acid solution. After homogenization, samples were centrifuged at 10 000 *g* for 10 min, supernatants were collected and its fluorescence was quantified using a spectrophotometer at an excitation wavelength of 620 nm and an emission wavelength of 680 nm. Dye in samples was determined as micrograms per gram of tissue from a standard curve plotted using known amounts of dye (Chen *et al.* 2008).

TUNEL staining

One and five days after injury, serial spinal cord sections (10 μm thickness) were collected every 100 μm and processed for terminal deoxynucleotidyl transferase-mediated deoxyuridine triphosphate-biotin nick end labeling (TUNEL) staining using an Apoptag *in situ* kit (Millipore, Billerica, MA, USA). Diaminobenzidine substrate kit (Vector Laboratories, Burlingame, CA, USA) was used for peroxidase staining, and the sections were then counter-stained with methyl green. Control sections were incubated in the absence of TdT enzyme. Investigators who were blind as to the experimental conditions carried out all TUNEL analyses. TUNEL-positive cells in the gray matter (GM) at 1 day (total 40 sections) and in the white matter (WM) at 5 days (total 100 sections) after SCI were counted and quantified using a 20 \times objective. Only those cells showing morphological features of nuclear condensation and/or compartmentalization in the GM and WM were counted as TUNEL-positive.

Western blot

Segments of spinal cord (1 cm) including the lesion site were isolated at indicated time points after SCI and total protein was prepared with a lysis buffer containing 1% Nonidet P-40, 20 mM Tris, pH 8.0, 137 mM NaCl, 0.5 mM EDTA, 10% glycerol, 10 mM $\text{Na}_2\text{P}_2\text{O}_7$, 10 mM NaF, 1 $\mu\text{g}/\text{mL}$ aprotinin, 10 $\mu\text{g}/\text{mL}$ leupeptin, 1 mM sodium vanadate, and 1 mM phenylmethanesulfonyl fluoride. Tissue homogenates were incubated for 20 min at 4°C, and centrifuged at 25 000 *g* for 30 min at 4°C. The protein concentration was determined using the BCA protein assay kit (Pierce, Rockford, IL, USA). Protein sample (40 μg) was separated on sodium dodecyl sulphate–polyacrylamide gel electrophoresis and

transferred to nitrocellulose membrane (Millipore). The membranes were blocked in 5% non-fat skim milk or 5% bovine serum albumin in tris-buffered saline and tween 20 (0.1%) for 1 h at 15–30°C followed by incubation with antibodies against cleaved occludin (1 : 500; Invitrogen), ZO-1 (1 : 500; Invitrogen), caspase 3 (1 : 1000; Cell Signaling Technology, Danvers, MA, USA), Akt (1 : 1000; Cell Signaling Technology), phosphorylated Akt (1 : 1000; Cell Signaling Technology), p53 (1 : 500; Cell Signaling Technology), acetylated histone-3 (Acetyl K9) (1 : 300; Abcam, Cambridge, MA, USA), myelin basic protein (MBP, 1 : 1000; Millipore), ED-1 (1 : 1000; Serotec, Raleigh, NC, USA) and heat-shock protein (HSP)-27 and -70 (1 : 500; Santa Cruz Biotechnology, Santa Cruz, CA, USA). The primary antibodies were detected with horseradish peroxidase-conjugated secondary antibodies (Jackson ImmunoResearch, West Grove, PA, USA). Immunoreactive bands were visualized by chemiluminescence using Supersignal (Thermo scientific, Rockford, IL, USA). β -Tubulin (1 : 10 000; Sigma) was used as an internal control. Experiments were repeated three times and the densitometric values of the bands on western blots obtained by AlphaImager software (Alpha Innotech Corporation) were subjected to statistical analysis. Background in films was subtracted from the optical density measurements.

Immunohistochemistry

Frozen sections were processed for immunohistochemistry with antibodies against myeloperoxidase (MPO, 1 : 100; Dako, Carpinteria, CA, USA) and ED-1 (1 : 300; Serotec, Raleigh, NC, USA) as previously described (Yune *et al.* 2007). After three washes in PBS for 5 min, sections were blocked in 5% normal serum and 0.1% Triton X-100 in PBS for 1 h at 15–30°C and then incubated with primary antibodies overnight at 4°C, followed by FITC-conjugated secondary antibodies (Jackson ImmunoResearch, West Grove, PA, USA). Nuclei were labeled with DAPI according to the protocol of the manufacturer (Molecular Probes, Eugene, OR, USA). In all controls, reaction to the substrate was absent if the primary antibody was omitted or if the primary antibody was replaced by a non-immune, control antibody. For quantification of MPO- or ED-1-positive cells, serial transverse sections (20 μm thickness) were collected ever 100 μm section rostral and caudal 3000 μm to the lesion site (total 60 sections). The number of MPO-positive neutrophils or ED-1-positive macrophages was expressed as a percentage relative to that in vehicle control (100%).

RNA isolation and RT-PCR

Total RNA was isolated using TRIZOL Reagent (Invitrogen) and 0.5 μg of total RNA was reverse-transcribed into first strand cDNA using MMLV according to the manufacturer's instructions (Invitrogen). For PCR amplifications, the following reagents were added to 1 μl of first strand cDNA: 0.5 U taq polymerase (Takara, Kyoto, Japan), 20 mM Tris–HCl, pH 7.9, 100 mM KCl, 1.5 mM MgCl_2 , 250 μM dNTP, and 10 pmole of each specific primer. PCR conditions were as follows: denaturation at 94°C, 30 s, primer annealing at indicated temperature, 30 s, and amplification at 72°C, 30 s. PCR was terminated by incubation at 72°C for 7 min. The primers used for MMP-2, MMP-9, Interleukin (IL)-1 β , IL-6, tumor necrosis factor α (TNF- α), cyclo-oxygenase-2 (COX-2), inducible nitric oxide synthase (iNOS) and GAPDH were synthesized by the Genotech (Daejeon, Korea) and the sequences of the primers are as

follows (5'–3'): MMP-2 forward, 5'-ACC ATC GCC CAT CAT CAA GT-3', MMP-2 reverse, 5'-CGA GCA AAA GCA TCA TCC AC-3' (348 bp, 55°C for 35 cycles); MMP-9 forward, 5'-AAA GGT CGC TCG GAT GGT TA-3', MMP-9 reverse, 5'-AGG ATT GTC TAC TGG AGT CGA-3' (698 bp, 55°C for 35 cycles); IL-1 β forward, 5'-GCA GCT ACC TAT GTC TTG CCC GTG-3', IL-1 β reverse, 5'-GTC GTT GCT TGT CTC TCC TTG TA-3' (289 bp, 50°C for 30 cycles); IL-6 forward, 5'-AAG TTT CTC TCC GCA AGA TAC TTC CAG CCA-3'; IL-6 reverse, 5'-AGG CAA ATT TCC TGG TTA TAT CCA GTT-3' (240 bp, 58°C for 30 cycles); TNF- α forward, 5'-CCC AGA CCC TCA CAC TCA GAT-3'; TNF- α reverse, 5'-TTG TCC CTT GAA GAG AAC CTG-3' (215 bp, 56°C for 28 cycles); COX-2 forward, 5'-CCA TGT CAA AAC CGT GGT GAA TG-3'; COX-2 reverse, 5'-ATG GGA GTT GGG CAG TCA TCA G-3' (374 bp, 55°C for 28 cycles); iNOS forward, 5'-CTC CAT GAC TCT CAG CAC AGA G-3'; iNOS reverse, 5'-GCA CCG AAG ATA TCC TCA TGA T-3' (401 bp, 56°C for 25 cycles); GAPDH forward, 5'-TCC CTC AAG ATT GTC AGC AA-3'; GAPDH, reverse, 5'-AGA TCC ACA ACG GAT ACA TT-3' (308 bp, 50°C for 23 cycles). The plateau phase of the PCR reaction was not reached under these PCR conditions. After amplification, PCR products were subjected to a 1.5% agarose gel electrophoresis and visualized by ethidium bromide staining. The relative density of bands (relative to sham value) was analyzed by the AlphaImager software (Alpha Innotech Corporation). Experiments were repeated three times and the values obtained for the relative intensity were subjected to statistical analysis. The gels shown in figures are representative of results from three separate experiments.

ELISA

The levels of cytokines (TNF- α , IL-1 β , and IL-6) were assayed using cytokine ELISA kits (BioSource Europe, Nivelles, Belgium). Rats were deeply anesthetized with chloral hydrate (500 mg/kg, i.p.) and cardinally perfused. The spinal cord was immediately removed after perfusion, weighed, and frozen in liquid nitrogen for storage at -80°C. For analysis of cytokines, tissues were homogenized and the levels of TNF- α , IL-1 β , and IL-6 were assayed by ELISA and determined according to the manufacturer's instructions. All samples were analyzed in triplicate.

Behavioral tests

Examination of functional deficits after injury was conducted as previously described (Yune *et al.* 2007). Trained investigators who were blind as to the experimental conditions performed behavioral analyses. To test hindlimb locomotor function, open-field locomotion was evaluated by using the Basso–Beattie–Bresnahan locomotion scale (Basso *et al.* 1995; Yune *et al.* 2007). The ability to control and place the hindlimb precisely was tested on a horizontal grid by counting the number of foot falls (mistake) in foot placing as previously described (Merkler *et al.* 2001). For footprint analysis, both animal's forepaws and hindpaws were dipped in red and blue dye (non-toxic) and then walked across a narrow box (1 m long and 7 cm wide) as previously described (Stirling *et al.* 2004). The footprints were scanned, and digitized images were analyzed.

Assessment of lesion volume

The measurement of lesion volume using rats tested for behavioral analysis was performed using serial longitudinal sections (10 μ m)

through the dorsoventral axis of the spinal cord as previously described (Yune *et al.* 2008a). Every 50 μ m section was stained with Cresyl violet acetate and studied with light microscopy. The rostrocaudal boundaries of the tissue damage were defined by the presence of inflammatory cells, the loss of neurons, the existence of degenerating neurons and cyst formation. With a low-power (1.25 \times) objective, the lesion area was determined by MetaMorph software (Molecular devices, Sunnyvale, CA, USA). Areas at each longitudinal level are determined, and the total lesion volume is derived by mean of numerical integration of sequential areas.

Statistical analysis

Data except behavior tests are presented as the mean \pm SD values and behavioral data are presented as the mean \pm SEM. Comparisons between vehicle and VPA treated groups were made by unpaired Student's *t*-test. Multiple comparisons between groups were performed one-way ANOVA. Behavioral scores from BBB analysis were analyzed by repeated measures ANOVA (time vs. treatment). Tukey's multiple comparison was used as *post hoc* analysis. Statistical significance was accepted with $p < 0.05$. Statistical analyses were performed using SPSS 15.0 (SPSS Science, Chicago, IL, USA).

Results

VPA inhibits matrix metalloprotease-9 expression and activity after SCI

As VPA is known to attenuate BBB disruption by inhibiting MMP-9 in an animal model of transient focal cerebral ischemia (Wang *et al.* 2011), we expected that VPA would inhibit MMP-9 after SCI. Rats were subjected to contusive spinal cord injury (SCI) at T9 level and killed at 1 day after injury. Total RNA and tissue extracts from spinal cord (10 mm) including lesion epicenter were prepared as described above. First, we examined MMP-2 and -9 mRNA expression at 1 day after injury by RT-PCR ($n = 3$). As shown in Fig. 1a, the levels of MMP-2 and -9 mRNA increased after injury. Notably, the increase in MMP-9 was much higher than in MMP-2. In addition, VPA significantly inhibited MMP-9 mRNA expression as compared with vehicle control, whereas MMP-2 mRNA expression was not significantly changed by the drug (Fig. 1a and b). Next, we analyzed MMP activity by gelatin zymography. MMP-2 and -9 activities also increased at 1 day after SCI (Fig. 1c and d) as reported (Noble *et al.* 2002; Choi *et al.* 2010). Furthermore, both MMP-2 and -9 activities were significantly inhibited by VPA. Especially, the decrease in MMP-9 activity by VPA was approximately fourfold and more pronounced when compared with that in MMP-2 ($n = 4$, MMP-9; Veh, 4.2 ± 0.2 vs. VPA, 1.2 ± 0.2 ; MMP-2; Veh, 3.0 ± 0.33 vs. VPA, 2.1 ± 0.34 , $p < 0.05$).

VPA attenuates blood–spinal cord barrier disruption after SCI

It is well known that SCI results in the breakdown of the BSCB (Noble and Wrathall 1989). As our results showed

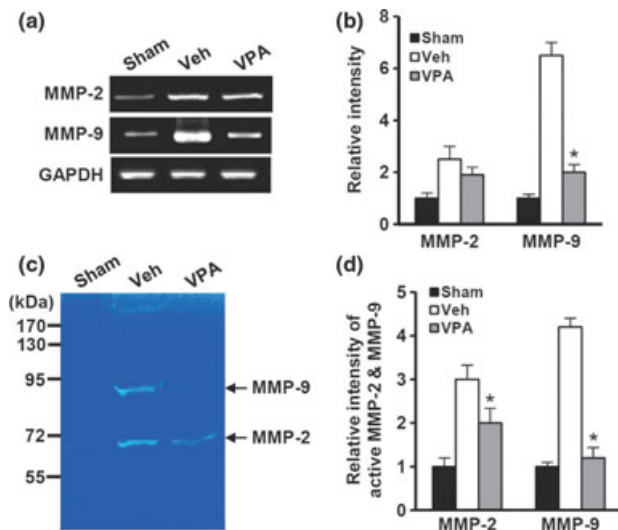


Fig. 1 VPA inhibits the expression and activity of MMP-9 after SCI. Rat receiving spinal contusion injury was administered immediately with VPA (300 mg/kg) and spinal cord tissues from 1 day after injury were processed for RT-PCR ($n = 3/\text{group}$), and gelatin zymography ($n = 4/\text{group}$) as described in the Methods section. (a) RT-PCR. (b) Densitometric analysis of RT-PCR. (c) Gelatin zymography. (d) Densitometric analysis of zymography. Data represent mean \pm SD. * $p < 0.05$ versus vehicle.

that VPA inhibited MMP-9, we anticipated that VPA would attenuate BSCB disruption. We examined the effect of VPA on BSCB disruption at 1 and 5 days after injury by Evans blue assay described in Method section ($n = 5$). As shown in Fig. 2 (Veh), SCI caused a profound increase in the amount of Evans blue dye extravasation as compared with uninjured sham control, indicating that injury elicits BSCB disruption. VPA significantly reduced the amount of Evans blue dye extravasation in a dose-dependent manner (150 and 300 mg/kg) at 1 and 5 days after injury as compared with vehicle control (Fig. 2b and d). Notably, the amount of Evans blue dye extravasation was reduced to closely the sham level by 300 $\mu\text{g}/\text{kg}$ of VPA at 5 days after injury (Fig. 2d). To obtain more clinically relevant evidence, we examined the effect of VPA on BSCB permeability after moderately severe SCI (50 gm-cm). Similar with moderate injury (25 gm-cm), VPA significantly inhibits the increase of BSCB permeability after severe injury (Fig. 2e and f). These data suggest that VPA can effectively prevent BSCB disruption by inhibiting MMP-9 activity after SCI.

VPA inhibits blood cell infiltration after SCI

It is known that BSCB is disrupted after SCI and blood infiltration such as neutrophils and macrophages is followed (Mun-Bryce and Rosenberg 1998a). As VPA prevents BSCB disruption after SCI (see Fig. 2a–f), we examined the effect of VPA treatment on the blood cells infiltration by immunohistochemistry against MPO for neutrophils and ED-1 for

macrophages and western blot for ED-1. As shown in Fig. 2g, infiltrated MPO-positive neutrophils and ED-1-positive macrophages were observed in the lesion site of injured spinal cord at 1 and 5 days respectively. In addition, the number of neutrophils and macrophages was significantly decreased in VPA-treated rat as compared with vehicle control (MPO: vehicle, $100 \pm 9.8\%$ vs. VPA, $56 \pm 9.1\%$; ED-1: vehicle, $100 \pm 7.0\%$ vs. VPA, $35 \pm 5.9\%$; $n = 5$, $p < 0.05$) (Fig. 2g and h). ED-1 expression in spinal cord lysates was also markedly increased after injury and VPA treatment significantly inhibited the ED-1 expression at 5 days as compared with vehicle control (Fig. 2i and j). These data suggest that VPA inhibits blood cell infiltration by preventing BSCB disruption after SCI.

VPA prevents loss of tight junction proteins after SCI

The tight junction (TJ) in the endothelial cells of blood vessel is involved in BBB integrity (Zlokovic 2008). To determine whether SCI-induced hyperpermeability was caused by TJ alterations, the expression of the TJ-associated proteins, occludin and ZO-1 was examined in spinal lysates by western blot. As shown in Fig. 3a, the antibodies against occludin and ZO-1 showed specific immunoreactivity at expected molecular weight proteins (65 kDa for occludin, 220 kDa for ZO-1). After injury, the levels of occludin and ZO-1 decreased (Fig. 3a) and the decrease was apparent at 1 and 3 days after injury (Fig. 3b). However, the level of ZO-1 returned nearly to the sham level at 5 and 7 days after injury (Fig. 3a and b). VPA-treated groups showed significantly higher levels of occludin and ZO-1 at 3 days after injury as compared with vehicle control (Fig. 3c and d), indicating that VPA prevents loss of TJ proteins after injury.

VPA reduces the expression of inflammatory mediators after SCI

It is known that after SCI, BSCB disruption followed blood infiltration mediates inflammation, thereby initiates the secondary injury cascade, by producing inflammatory mediators such as IL-1 β , IL-6, TNF- α , COX-2 and iNOS (Mun-Bryce and Rosenberg 1998b). Therefore, we postulated that VPA treatment would inhibit the production of inflammatory mediators after injury. We examined the expression of mediators by RT-PCR, western blot and ELISA after injury. The levels of TNF- α , IL-1 β (at 2 h), IL-6, iNOS and COX-2 (at 6 h) mRNA increased after injury, which were significantly decreased by VPA ($n = 3$) (Fig. 4a and b). ELISA assays also showed that VPA significantly inhibited the production of TNF- α , IL-1 β , and IL-6 at 1 day after injury (TNF- α , IL-1 β , and IL-6 of vehicle group: 55 ± 5.0 , 65 ± 3.0 , 41 ± 4.1 pg/mL vs. VPA group: 32 ± 1.5 , 38 ± 2.0 , 28 ± 3.0 pg/mL respectively; $n = 5$, $p < 0.05$) (Fig. 4c). By western blot, the protein levels of iNOS and COX-2 at 1 day after injury were significantly decreased by VPA as compared with vehicle control ($n = 5$, $p < 0.05$) (Fig. 4d and e).

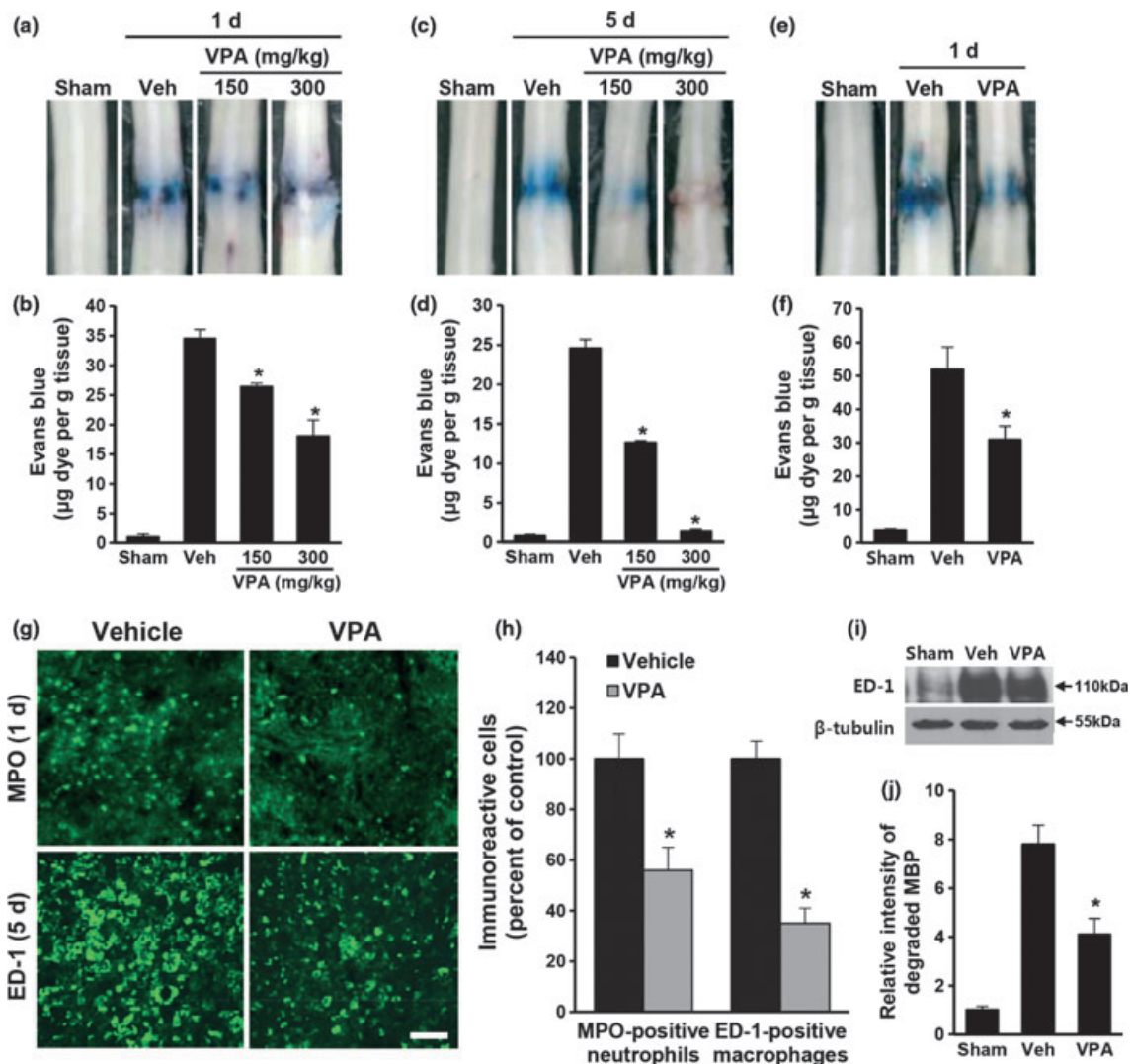


Fig. 2 VPA attenuates BSCB disruption and blood infiltration after SCI. After SCI (25 or 50 gm-cm), rats were treated with VPA (150 or 300 mg/kg). BSCB permeability was measured by using Evans blue dye and blood infiltration was assessed by counting the MPO or ED-1-labeled cells at 1 and 5 days or western blot for ED-1 at 5 days after injury as described in the Methods section ($n = 5/\text{group}$). Representative spinal cord showing Evans blue dye permeabilized into moderately injured (25 gm-cm) spinal cord at 1 (a) and 5 days (c) and quantification of the amount of Evans blue at 1 (b) and 5 days (d) after injury. (e) Evans blue injected spinal cord from vehicle or VPA (300 mg/kg)-treated rats at 1 day after mod-

erately severe SCI (50 gm-cm). (f) Quantification of the Evans blue extravasation. (g) Photomicrographs from MPO-labeled neutrophils or ED-1-labeled macrophages in animals injected with vehicle (left panel) or VPA (300 mg/kg, right panel). The representative sections were obtained at 2 mm rostral to lesion epicenter. Scale bar, 50 µm. (h) Quantitative analysis of MPO- or ED-1-positive cells. (i) Western blot of ED-1 at 5 days after injury (j) Densitometric analyses of western blots show that VPA (300 mg/kg) significantly inhibited ED-1 expression when compared with that observed in vehicle control at 5 days after injury. Data represent mean \pm SD. * $p < 0.05$ versus vehicle.

VPA inhibits apoptotic cell death after SCI

VPA is known to exert neuroprotective effects in various neurological diseases such as ischemia, amyotrophic lateral sclerosis, and SCI (Kim *et al.* 2007; Qian *et al.* 2010). Thus, we hypothesized that VPA would inhibit cell death of neurons and oligodendrocytes after SCI. By TUNEL staining, we examined the effect of VPA on apoptotic cell death at 1 day in the GM and at 5 days in the WM after SCI. Serial transverse

sections (10 µm thickness) were collected every 100 µm from 2 mm rostral to 2 mm caudal to the lesion epicenter (total 40 sections for neurons) or 5 mm rostral to 5 mm caudal to the lesion epicenter (total 100 sections for oligodendrocytes). TUNEL-positive cells were observed mostly near and within the lesion area in the GM at 1 day and in the WM at 5 days mostly outside of the lesion area extending the entire length of the section (10 mm) (Fig. 5a). Our previous reports (Yune

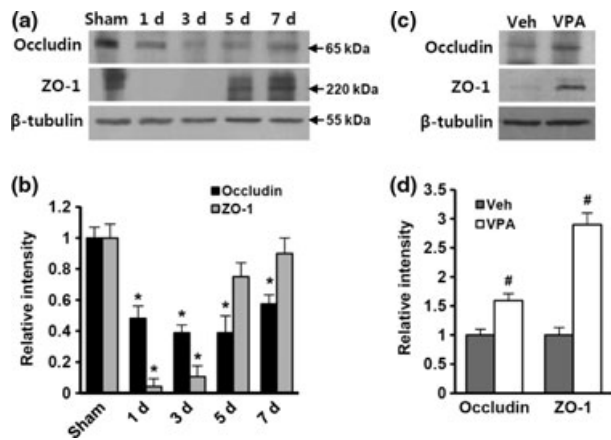


Fig. 3 VPA prevents the degradation of tight junction proteins after SCI. To examine the degradation of tight junction proteins after SCI, rats were treated with VPA (300 mg/kg) and total spinal extracts from injured spinal cord at indicated time points as described in the Methods section ($n = 3/\text{group}$). Western blots of occludin and ZO-1 at time point after injury (a) and after VPA treatment (c). (b, d) Densitometric analyses of western blot. Data represent mean \pm SD. * $p < 0.05$ versus sham, # $p < 0.05$ versus vehicle.

et al. 2009; Lee *et al.* 2010) demonstrate that by double-labeling, most TUNEL-positive cells in the GM are neurons at 1 day and oligodendrocytes in the WM at 5 days after injury (data not shown). VPA (300 mg/kg) significantly decreased the number of TUNEL-positive neurons and oligodendrocytes when compared with the vehicle-treated control ($n = 5$, Vehicle, 392 ± 19 vs. VPA, 190 ± 8 cells for neurons; Vehicle, 256 ± 15 vs. VPA, 115 ± 3 cells for oligodendrocytes, $p < 0.05$) (Fig. 5b). In addition, the level of cleaved

(activated) forms of caspase 3 increased at 4 h and 5 days after injury as we previously reported (Lee *et al.* 2010) and VPA treatment significantly decreased the level of activated caspase 3 at both 4 h and 5 days after injury when compared with vehicle control (Fig. 5c and d) (Vehicle, 3.9 ± 0.23 vs. VPA, 2.6 ± 0.13 at 4 h, Vehicle, 4.5 ± 0.15 vs. VPA, 2.3 ± 0.1 at 5 days, $n = 3$, $p < 0.05$). Thus, our results indicate that VPA inhibits apoptotic cell death of neurons and oligodendrocytes after injury.

It is also known that MBP is one of the substrates of MMP-9 (Chandler *et al.* 1995; Kobayashi *et al.* 2008). As VPA inhibited MMP-9 activity and oligodendrocyte cell death after SCI (see Figs 1 and 5), we expected that VPA treatment would protect white matter structures. By western blot, four isoforms of MBP (21.5, 18.5, 17 and 14 kDa) was detected and the degraded band (approximate 10 kDa) was appeared in injured spinal cord as previous report (Lin *et al.* 2007). Densitometric analysis revealed that the level of degraded MBP was significantly reduced in VPA-treated rats as compared with vehicle control (Fig. 5e and f).

VPA up-regulates the levels of acetylated histone H3, proteins related to anti-apoptotic function after injury

VPA exerts neuroprotective effects by increasing the level of acetylated histone H3 (Acetyl-H3 at lys9) after transient focal cerebral ischemia (Ren *et al.* 2004). In addition, Penas *et al.* (2011) show that VPA prevents oligodendrocyte cell death and axon loss by up-regulating the level of Acetyl-H3 after SCI. Thus, we expected that VPA would increase Acetyl-H3 level after injury. We measured the levels of Acetyl-H3 as an index of HDAC inhibition in injured spinal cord. The level of Acetyl-H3 increased and peaked at 3 days after injury

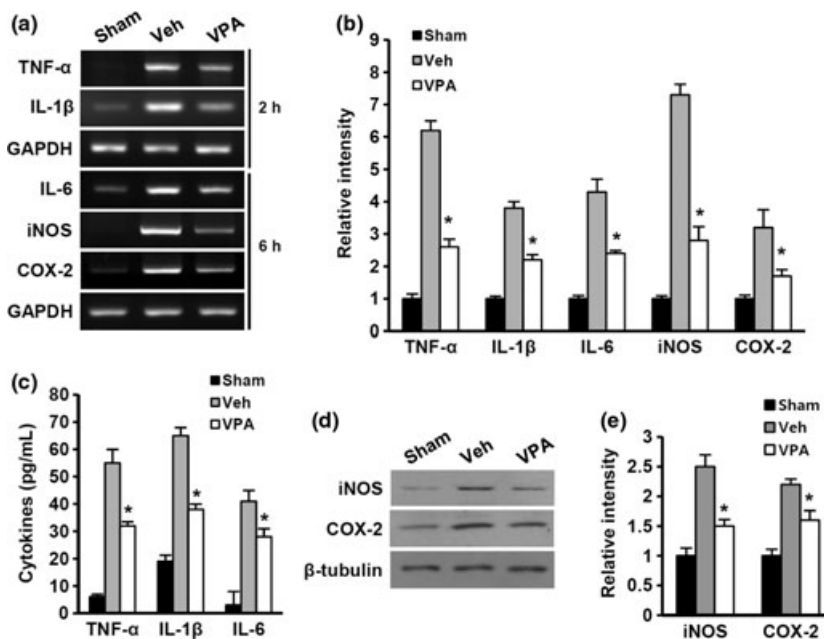


Fig. 4 VPA inhibits the expression and production of inflammatory mediators after SCI. Total RNA and spinal extracts from vehicle or VPA-treated samples at indicated time points after injury were prepared as described in the Methods section. (a) RT-PCR of TNF- α , IL-1 β (at 2 h), IL-6, COX-2 and iNOS (at 6 h) after injury ($n = 3/\text{group}$). (b) Quantitative analysis of RT-PCR. (c) ELISA assay of TNF- α , IL-1 β , IL-6 at 1 day after injury ($n = 5/\text{group}$). (d) Western blots of iNOS and COX-2 at 1 day after injury ($n = 5/\text{group}$). (e) Quantitative analysis of western blots. Data represent mean \pm SD. * $p < 0.05$ versus vehicle.

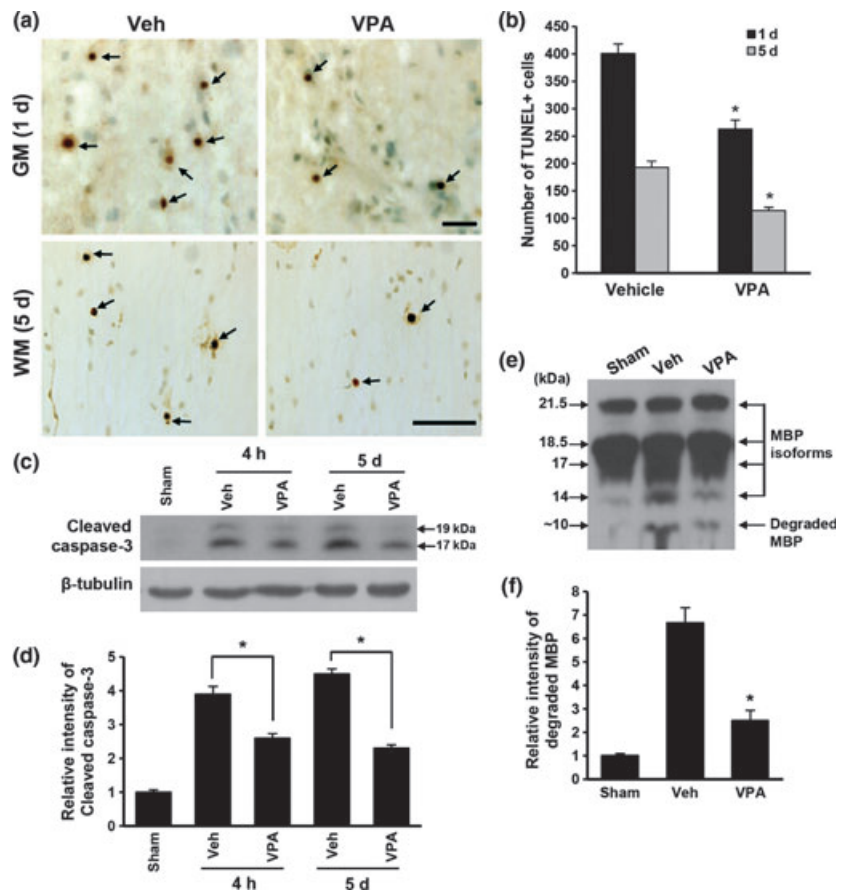


Fig. 5 VPA inhibits apoptotic cell death after SCI. After SCI, rats were treated with VPA (300 mg/kg) and spinal tissues (at 1 and 5 days) and extracts (at 4 h, 3 days and 5 days) were prepared for TUNEL staining and western blot as described in the Methods section. (a) Representative images of TUNEL staining. Scale bars, 50 μ m. (b) Quantitative analysis of TUNEL-positive cells ($n = 5$ /group). (c) Western blots of caspase 3. (d) Densitometric analysis of western blots ($n = 3$ /group). (e) Western blot for MBP at 3 days after injury. (f) Densitometric analysis of western blot ($n = 3$ /group). Values are mean \pm SD. * $p < 0.05$ versus vehicle.

(Fig. 6a). VPA significantly increased the level of Acetyl-H3 when compared with vehicle control ($n = 3$, VPA, 4.3 ± 0.2 vs. Veh, 2.2 ± 0.2 , $p < 0.05$) (Fig. 6b and c). Treatment of

normal rats with VPA also elicited an increase in the level of Acetyl-H3 (data not shown). However, levels of acetylation of histone H2, H4 were not affected by VPA (data not

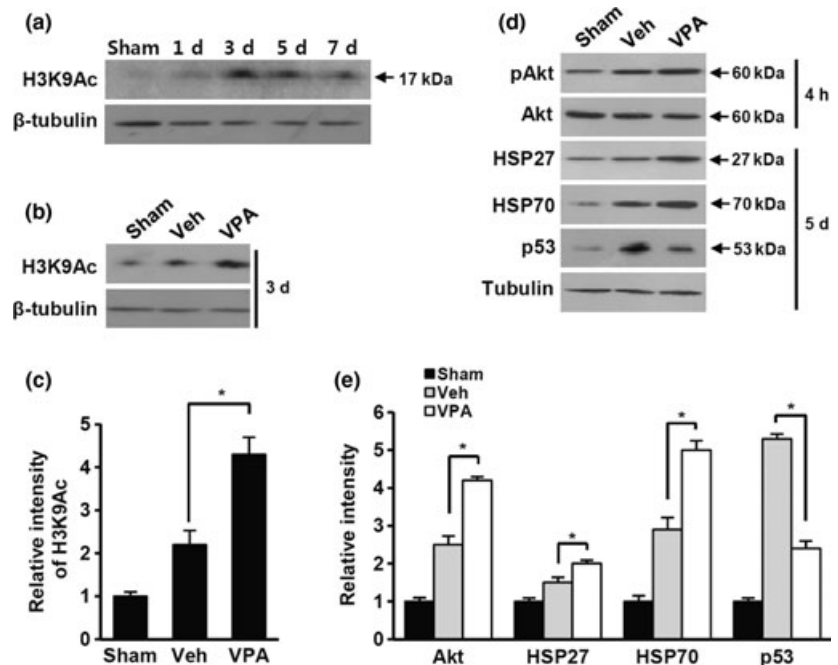


Fig. 6 VPA up-regulates the levels of acetylated histone 3 (H3K9Ac) and anti-apoptotic proteins expression after SCI. Total extracts from injured spinal cord with or without VPA treatment at indicated time points after injury were prepared as described in the Methods section ($n = 3$ /group). (a) Western blot of acetylated histone 3 (H3K9Ac) after injury. (b) Effect of VPA on H3K9Ac. (c) Quantitative analysis western blot. (d) Western blots of pAkt, Akt (4 h), HSP27, HSP70, p53 (5 days) after SCI. (e) Quantitative analysis of western blots. Values are mean \pm SD. * $p < 0.05$ versus vehicle.

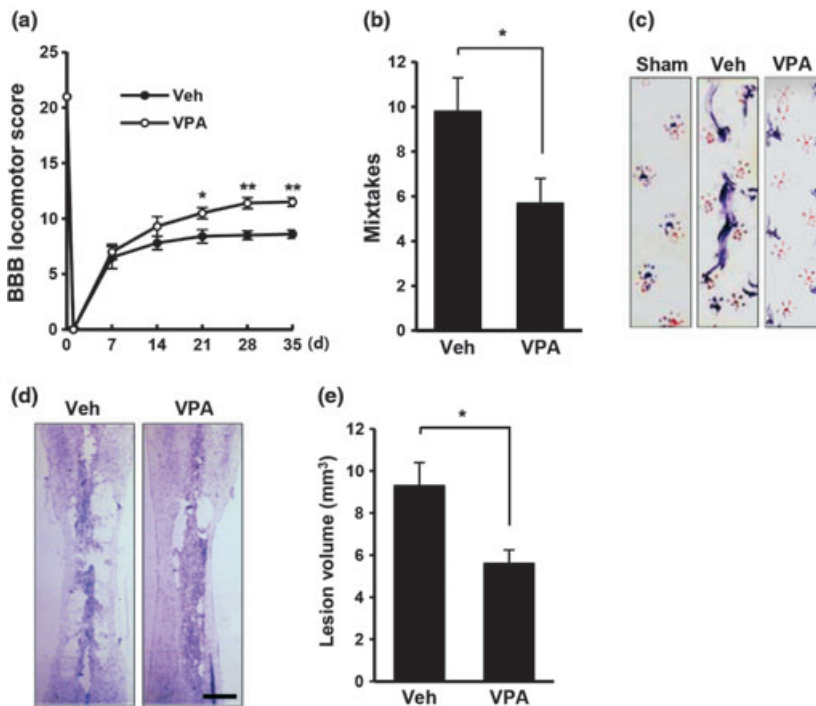


Fig. 7 VPA improves functional recovery and reduces lesion volume after SCI. After SCI, rats were treated with VPA (300 mg/kg) and functional recovery was assessed with the BBB test, grid walk test, and footprint analysis after injury ($n = 7/\text{group}$). Each value represents the mean \pm SEM obtained from 15 animals. (a) BBB scores. (b) Grid walk test. (c) Representative footprints obtained from each group at 35 days after SCI. (d) Representative spinal cord tissues (1.2 mm from dorsal surface) showing cavitation in the lesion site at 38 days after injury. Scale bar, 1 mm. (e) Quantitative analysis of lesion volumes. Data are presented as mean \pm SD. * $p < 0.05$, ** $p < 0.01$ versus vehicle.

shown). These data suggest that the neuroprotective effect of VPA may be mediated in part by increasing the acetylation of histone H3 after SCI.

VPA is also known to up-regulate the level of p-Akt and HSP70, and down-regulates p53 level in an ischemic model (Ren *et al.* 2004; Kim *et al.* 2007). We examined the changes in levels of cytoprotective and apoptotic proteins by VPA by western blot. As shown in Fig. 6d, the level of pAkt (at 4 h), HSP27, HSP70 and p53 (at 5 days) increased after injury. In addition, VPA significantly further increased the level of pAkt, HSP27, and HSP70 expression, whereas the level of p53 was decreased by VPA when compared with vehicle control (Fig. 6d and e, $n = 3$). However, VPA did not change the levels of pAkt, HSP27, HSP70 and p53 in uninjured spinal cord (data not shown). These results suggest that the neuroprotective effect of VPA may be mediated in part by increasing pAkt, HSP27 and HSP70 and decreasing p53 expression after SCI.

VPA improves functional recovery after SCI

Injured rats were treated with VPA (300 mg/kg) twice a day for five consecutive days. Functional recovery was then evaluated for 5 weeks after injury using the Basso–Beattie–Bresnahan rating scale, grid walk and footprint recordings. As results, VPA significantly increased the hindlimb locomotor function, 21–35 days after injury as compared with that observed in vehicle-treated control ($n = 15/\text{group}$, 35 days, VPA, 11.5 ± 0.4 vs. Vehicle, 8.6 ± 0.37 , $p < 0.01$) (Fig. 7a). The ability to control and place the hindlimbs precisely was tested on a horizontal grid at

35 days after injury. The number of mistakes (footfalls on the grid walk) in VPA-treated groups was significantly lower than vehicle-treated group (VPA, 5.7 ± 1.1 vs. Vehicle, 9.8 ± 1.5 , $p < 0.05$) (Fig. 7b). Footprint analyses at 35 days after SCI indicate that VPA-treated rats showed fairly consistent forelimb–hindlimb coordination and very little toe dragging. By contrast, vehicle-treated animals showed inconsistent coordination and extensive drags as revealed by ink streaks extending from both hindlimbs (Fig. 7c).

Traumatic injury to the spinal cord also triggers immediate mechanical damage, followed by a secondary cascade of degenerative processes, leading to progressive tissue loss (Schwab and Bartholdi 1996; Lee *et al.* 2003). When tissue loss with serial longitudinal sections after Cresyl violet staining was evaluated, the total lesion volume was significantly decreased upon VPA as compared with that of vehicle treatment (VPA, 5.6 ± 0.65 vs. Vehicle, $9.3 \pm 1.1 \text{ mm}^3$, $p < 0.05$) (Fig. 7e).

Discussion

The present study shows that the neuroprotective effect of VPA might be mediated in part by attenuating BSCB disruption via inhibition of MMP-9 activity after SCI. We also demonstrated that post-injury treatment with VPA inhibited apoptotic cell death of neurons and oligodendrocytes and improved functional recovery after SCI. Furthermore, the present study showed that the neuroprotective effect of VPA might also be mediated in part by modulating the production of inflammatory mediators, the level of

acetylated histone 3 (acetyl-H3 at lys9) and up-regulating anti-apoptotic molecules such as pAkt, HSP27, HSP70 and down-regulating p53 after injury. Based on our results, it is likely that multiple signaling pathways may be involved in the neuroprotective effect of VPA after SCI.

VPA is a short-chain fatty acid that readily crosses the BBB and has low toxicity and acceptable tolerability in both human and animal studies (Nalivaeva *et al.* 2009; Biermann *et al.* 2011). In this study, VPA (300 mg/kg) was administered by subcutaneous injection twice daily for 5 days. This dosage was close to that used to control seizure in rats, and was the same that found to exert neuroprotective effects against cerebral ischemia (Ren *et al.* 2004; Kim *et al.* 2007), intracerebral hemorrhage (Sinn *et al.* 2007) and malonate-induced toxicity (Morland *et al.* 2004). In addition, we did not observe any significant change in body weight among the experimental groups (data not shown) during our experiment. Also, neither significant side effects nor an increase in mortality by VPA treatment were observed.

Up-regulation of MMP-9 has been implicated in SCI-induced secondary damage and BSCB disruption by degrading the basal components of BBB and facilitating immune cell infiltration (Noble *et al.* 2002). Our results also show that MMP-9 expression was up-regulated and its enzyme activity was increased at 1 day after SCI. Furthermore, VPA treatment significantly decreased the expression and gelatinase activity of MMP-9 at 1 day after SCI (see Fig. 1). This result is consistent with a previous report showing that VPA attenuates ischemia-induced BBB disruption and brain edema by inhibiting MMP-9 induction and tight junction degradation (Wang *et al.* 2011). It is also known that MMP-9 degrades gelatin, collagens (type IV, V, and XI), elastin, vitronectin, myelin-basic protein, and other substrates (Vu and Werb 2000). In addition, tight junction proteins as essential components of BBB or BSCB are known to be substrate of MMP (Yang *et al.* 2007). As shown in Fig. 3a, tight junction proteins, occludin and ZO-1, was degraded after SCI and VPA significantly inhibited degradation of these molecules (Fig. 3c). Furthermore, BBB disruption induced by transient focal cerebral ischemia is attenuated in MMP-9 knockout mice by reducing degradation of ZO-1 protein as compared with wild type mice (Asahi *et al.* 2001). Thus, these results indicate that VPA prevents BSCB disruption by reducing degradation of tight junction proteins via inhibition of MMP-9 activity after SCI. Nevertheless, MMP-2 is also known to be up-regulated after SCI and contribute to apoptotic cell death (Dang *et al.* 2008). In fact, our results show that MMP-2 increased after injury and VPA significantly inhibited MMP-2 activity (see Fig. 1). Thus, we can't rule out the possibility that the protective effect of VPA on BSCB function can also be mediated by inhibiting MMP-2 activity after SCI.

Extensive evidences show that inflammatory cells such as neutrophils and macrophages are infiltrated via BSCB disruption, increase tissue damage, induce apoptotic cell

death, and impair functional recovery after injury (Carlson *et al.* 1998; Beattie *et al.* 2000; Popovich *et al.* 2003; Okada *et al.* 2004). Our data also show that the expression of inflammatory mediators such as TNF- α , IL-1 β , IL-6, iNOS, and COX-2, up-regulated after SCI. In parallel with this result, apoptotic cell death increased in the GM and WM after injury (see Fig. 5). Furthermore, VPA significantly inhibited the expression of inflammatory mediators and apoptotic cell death (see Fig. 5), and improved functional recovery after SCI (see Fig. 7). Carlson *et al.* (1998) showed that the number of infiltrating neutrophils significantly correlates with the amount of tissue damage after SCI. Several studies also demonstrated that suppression of neutrophil and macrophage infiltration after injury ameliorates apoptotic cell death and improves functional recovery (Hamada *et al.* 1996; Taoka *et al.* 1997; Saiwai *et al.* 2010). Thus, our results suggest that the neuroprotective effect of VPA might be mediated by attenuating BSCB disruption, thereby prevent the infiltration of neutrophils and macrophages after SCI, although we did not examine the effect of VPA on the infiltration of blood cells in this study.

After SCI, the level of Acetyl-H3 increased (see Fig. 6a) as reported (Penas *et al.* 2011). The increased histone acetylation in injured rat spinal cords could be due to inactivation of HDAC or activation of histone acetyltransferase. Our data suggest that the increase of Acetyl-H3 level by VPA treatment (see Fig. 6b and c) is likely caused by the inhibition of HDAC activity by VPA. Hyperacetylation of histones at lysine residues weakens the interaction of histone with DNA, leading to relaxation of the nucleosome structure and facilitation of transcription factor binding to DNA elements (Berger 1999). Our data show that VPA increased the expression of HSP27, HSP70, and phosphorylation of Akt, which are known to function as survival factors after SCI and ischemia (see Fig. 6d and e) (Lee *et al.* 2004; Yune *et al.* 2008b; van der *et al.* 2010). However, VPA attenuated the increase of p53 level (Saito *et al.* 2000; Kotipatruni *et al.* 2011), which is known to be involved in apoptotic cell death after SCI. Taken together, our data suggest that VPA might also exert its neuroprotective effect in part by modulating the expression of HSP27, HSP70, and p53, and phosphorylating Akt under epigenetic control after SCI. Additional studies are necessary to uncover the VPA-associated epigenetic control mechanisms and the VPA-targeted genes and transcription factors after SCI.

We have examined the effect of VPA on MMP-9 expression and activity after SCI. As shown in this study, VPA attenuates BSCB disruption by inhibiting MMP-9 activity and improves functional recovery after SCI. Thus, our findings are consistent with a report (Wang *et al.* 2011) showing that VPA reduces BBB disruption by inhibiting MMP-9 in a rat model of ischemia. VPA is currently used for the treatment of seizures and bipolar mood disorder (Tunnicliff 1999; Johannessen 2000). Considering the

neuroprotective effects of VPA in the animal models of CNS injury and diseases (Kim *et al.* 2007; Sinn *et al.* 2007; Qian *et al.* 2010; Lv *et al.* 2011), our results suggest that VPA may provide effective therapeutic interventions for preventing BSCB disruption and for improving functional outcome after SCI. Thus, understanding the mechanism of action of VPA will assist in the development of more potent analogues for treatment of human SCI.

Acknowledgements

This study was supported by grants from the Ministry of Education, Science and Technology (MEST), the Republic of Korea. [No. 2011K000282, 2011K000291 (Brain Research Center of the 21st Century Frontier Research Program), 20110001692 (Pioneer Research Center Program), 20110000932 (Basic Science Research Program), KRF-2007-331-E00199]. The authors declare no conflict of interest.

References

- Abbott N. J., Ronnback L. and Hansson E. (2006) Astrocyte-endothelial interactions at the blood-brain barrier. *Nat. Rev. Neurosci.* **7**, 41–53.
- Asahi M., Wang X., Mori T., Sumii T., Jung J. C., Moskowitz M. A., Fini M. E. and Lo E. H. (2001) Effects of matrix metalloproteinase-9 gene knock-out on the proteolysis of blood-brain barrier and white matter components after cerebral ischemia. *J. Neurosci.* **21**, 7724–7732.
- Basso D. M., Beattie M. S. and Bresnahan J. C. (1995) A sensitive and reliable locomotor rating scale for open field testing in rats. *J. Neurotrauma* **12**, 1–21.
- Beattie M. S., Farooqui A. A. and Bresnahan J. C. (2000) Review of current evidence for apoptosis after spinal cord injury. *J. Neurotrauma* **17**, 915–925.
- Berger S. L. (1999) Gene activation by histone and factor acetyltransferases. *Curr. Opin. Cell Biol.* **11**, 336–341.
- Biermann J., Boyle J., Pielon A. and Lagreze W. A. (2011) Histone deacetylase inhibitors sodium butyrate and valproic acid delay spontaneous cell death in purified rat retinal ganglion cells. *Mol. Vis.* **17**, 395–403.
- Carlson S. L., Parrish M. E., Springer J. E., Doty K. and Dossett L. (1998) Acute inflammatory response in spinal cord following impact injury. *Exp. Neurol.* **151**, 77–88.
- Chandler S., Coates R., Gearing A., Lury J., Wells G. and Bone E. (1995) Matrix metalloproteinases degrade myelin basic protein. *Neurosci. Lett.* **201**, 223–226.
- Chang K. T. and Min K. T. (2002) Regulation of lifespan by histone deacetylase. *Ageing Res. Rev.* **1**, 313–326.
- Chen X., Lan X., Roche I., Liu R. and Geiger J. D. (2008) Caffeine protects against MPTP-induced blood-brain barrier dysfunction in mouse striatum. *J. Neurochem.* **107**, 1147–1157.
- Choi D. C., Lee J. Y., Moon Y. J., Kim S. W., Oh T. H. and Yune T. Y. (2010) Acupuncture-mediated inhibition of inflammation facilitates significant functional recovery after spinal cord injury. *Neurobiol. Dis.* **39**, 272–282.
- Dang A. B., Tay B. K., Kim H. T., Nauth A., fonso-Jaume M. A. and Lovett D. H. (2008) Inhibition of MMP2/MMP9 after spinal cord trauma reduces apoptosis. *Spine (Phila Pa 1976)* **33**, E576–E579.
- Feng L., Tang W. W., Loskutoff D. J. and Wilson C. B. (1993) Dysfunction of glomerular fibrinolysis in experimental antiglomerular basement membrane antibody glomerulonephritis. *J. Am. Soc. Nephrol.* **3**, 1753–1764.
- Gerzanich V., Woo S. K., Vennekens R. *et al.* (2009) De novo expression of Trpm4 initiates secondary hemorrhage in spinal cord injury. *Nat. Med.* **15**, 185–191.
- Gottlicher M., Minucci S., Zhu P. *et al.* (2001) Valproic acid defines a novel class of HDAC inhibitors inducing differentiation of transformed cells. *EMBO J.* **20**, 6969–6978.
- Hamada Y., Ikata T., Katoh S., Nakauchi K., Niwa M., Kawai Y. and Fukuzawa K. (1996) Involvement of an intercellular adhesion molecule 1-dependent pathway in the pathogenesis of secondary changes after spinal cord injury in rats. *J. Neurochem.* **66**, 1525–1531.
- Hawkins B. T. and Davis T. P. (2005) The blood-brain barrier/neurovascular unit in health and disease. *Pharmacol. Rev.* **57**, 173–185.
- Johannessen C. U. (2000) Mechanisms of action of valproate: a commentary. *Neurochem. Int.* **37**, 103–110.
- Kim H. J., Rowe M., Ren M., Hong J. S., Chen P. S. and Chuang D. M. (2007) Histone deacetylase inhibitors exhibit anti-inflammatory and neuroprotective effects in a rat permanent ischemic model of stroke: multiple mechanisms of action. *J. Pharmacol. Exp. Ther.* **321**, 892–901.
- Kobayashi H., Chattopadhyay S., Kato K., Dolkas J., Kikuchi S., Myers R. R. and Shubayev V. I. (2008) MMPs initiate Schwann cell-mediated MBP degradation and mechanical nociception after nerve damage. *Mol. Cell. Neurosci.* **39**, 619–627.
- Kotipatruni R. R., Dasari V. R., Veeravalli K. K., Dinh D. H., Fassett D. and Rao J. S. (2011) p53- and Bax-mediated apoptosis in injured rat spinal cord. *Neurochem. Res.* **36**, 2063–2074.
- Lee S. M., Yune T. Y., Kim S. J., Park D. W., Lee Y. K., Kim Y. C., Oh Y. J., Markelonis G. J. and Oh T. H. (2003) Minocycline reduces cell death and improves functional recovery after traumatic spinal cord injury in the rat. *J. Neurotrauma* **20**, 1017–1027.
- Lee S. H., Kwon H. M., Kim Y. J., Lee K. M., Kim M. and Yoon B. W. (2004) Effects of hsp70.1 gene knockout on the mitochondrial apoptotic pathway after focal cerebral ischemia. *Stroke* **35**, 2195–2199.
- Lee J. Y., Chung H., Yoo Y. S., Oh Y. J., Oh T. H., Park S. and Yune T. Y. (2010) Inhibition of apoptotic cell death by ghrelin improves functional recovery after spinal cord injury. *Endocrinology* **151**, 3815–3826.
- Lin Y., Vreman H. J., Wong R. J., Tjoa T., Yamauchi T. and Noble-Haeusslein L. J. (2007) Heme oxygenase-1 stabilizes the blood-spinal cord barrier and limits oxidative stress and white matter damage in the acutely injured murine spinal cord. *J. Cereb. Blood Flow Metab.* **27**, 1010–1021.
- Lv L., Sun Y., Han X., Xu C. C., Tang Y. P. and Dong Q. (2011) Valproic acid improves outcome after rodent spinal cord injury: Potential roles of histone deacetylase inhibition. *Brain Res.* **1396**, 60–68.
- Merkler D., Metz G. A., Raineteau O., Dietz V., Schwab M. E. and Fouad K. (2001) Locomotor recovery in spinal cord-injured rats treated with an antibody neutralizing the myelin-associated neurite growth inhibitor Nogo-A. *J. Neurosci.* **21**, 3665–3673.
- Morland C., Boldingh K. A., Iversen E. G. and Hassel B. (2004) Valproate is neuroprotective against malonate toxicity in rat striatum: an association with augmentation of high-affinity glutamate uptake. *J. Cereb. Blood Flow Metab.* **24**, 1226–1234.
- Mun-Bryce S. and Rosenberg G. A. (1998a) Gelatinase B modulates selective opening of the blood-brain barrier during inflammation. *Am. J. Physiol.* **274**, R1203–R1211.
- Mun-Bryce S. and Rosenberg G. A. (1998b) Matrix metalloproteinases in cerebrovascular disease. *J. Cereb. Blood Flow Metab.* **18**, 1163–1172.

- Nalivaeva N. N., Belyaev N. D. and Turner A. J. (2009) Sodium valproate: an old drug with new roles. *Trends Pharmacol. Sci.* **30**, 509–514.
- Noble L. J. and Wrathall J. R. (1989) Distribution and time course of protein extravasation in the rat spinal cord after contusive injury. *Brain Res.* **482**, 57–66.
- Noble L. J., Donovan F., Igarashi T., Goussev S. and Werb Z. (2002) Matrix metalloproteinases limit functional recovery after spinal cord injury by modulation of early vascular events. *J. Neurosci.* **22**, 7526–7535.
- Okada S., Nakamura M., Mikami Y. *et al.* (2004) Blockade of interleukin-6 receptor suppresses reactive astrogliosis and ameliorates functional recovery in experimental spinal cord injury. *J. Neurosci. Res.* **76**, 265–276.
- Penas C., Verdu E., sensio-Pinilla E., Guzman-Lenis M. S., Herrando-Grabulosa M., Navarro X. and Casas C. (2011) Valproate reduces CHOP levels and preserves oligodendrocytes and axons after spinal cord injury. *Neuroscience* **178**, 33–44.
- Phiel C. J., Zhang F., Huang E. Y., Guenther M. G., Lazar M. A. and Klein P. S. (2001) Histone deacetylase is a direct target of valproic acid, a potent anticonvulsant, mood stabilizer, and teratogen. *J. Biol. Chem.* **276**, 36734–36741.
- Popovich P. G., van R. N., Hickey W. F., Preidis G. and McGaughy V. (2003) Hematogenous macrophages express CD8 and distribute to regions of lesion cavitation after spinal cord injury. *Exp. Neurol.* **182**, 275–287.
- Qian Y. R., Lee M. J., Hwang S., Kook J. H., Kim J. K. and Bae C. S. (2010) Neuroprotection by valproic Acid in mouse models of permanent and transient focal cerebral ischemia. *Korean J. Physiol. Pharmacol.* **14**, 435–440.
- Ren M., Leng Y., Jeong M., Leeds P. R. and Chuang D. M. (2004) Valproic acid reduces brain damage induced by transient focal cerebral ischemia in rats: potential roles of histone deacetylase inhibition and heat shock protein induction. *J. Neurochem.* **89**, 1358–1367.
- Rosenberg G. A. and Navratil M. (1997) Metalloproteinase inhibition blocks edema in intracerebral hemorrhage in the rat. *Neurology* **48**, 921–926.
- Rosenberg G. A., Dencoff J. E., McGuire P. G., Liotta L. A. and Stetler-Stevenson W. G. (1994) Injury-induced 92-kilodalton gelatinase and urokinase expression in rat brain. *Lab. Invest.* **71**, 417–422.
- Rosenberg G. A., Estrada E. Y. and Dencoff J. E. (1998) Matrix metalloproteinases and TIMPs are associated with blood-brain barrier opening after reperfusion in rat brain. *Stroke* **29**, 2189–2195.
- Saito N., Yamamoto T., Watanabe T., Abe Y. and Kumagai T. (2000) Implications of p53 protein expression in experimental spinal cord injury. *J. Neurotrauma* **17**, 173–182.
- Saiwai H., Ohkawa Y., Yamada H., Kumamaru H., Harada A., Okano H., Yokomizo T., Iwamoto Y. and Okada S. (2010) The LTB4-BLT1 axis mediates neutrophil infiltration and secondary injury in experimental spinal cord injury. *Am. J. Pathol.* **176**, 2352–2366.
- Schwab M. E. and Bartholdi D. (1996) Degeneration and regeneration of axons in the lesioned spinal cord. *Physiol. Rev.* **76**, 319–370.
- Sinn D. I., Kim S. J., Chu K. *et al.* (2007) Valproic acid-mediated neuroprotection in intracerebral hemorrhage via histone deacetylase inhibition and transcriptional activation. *Neurobiol. Dis.* **26**, 464–472.
- Sternlicht M. D. and Werb Z. (2001) How matrix metalloproteinases regulate cell behavior. *Annu. Rev. Cell Dev. Biol.* **17**, 463–516.
- Sternlicht M. D., Lochter A., Sympon C. J., Huey B., Rougier J. P., Gray J. W., Pinkel D., Bissell M. J. and Werb Z. (1999) The stromal proteinase MMP3/stromelysin-1 promotes mammary carcinogenesis. *Cell* **98**, 137–146.
- Stirling D. P., Khodarahmi K., Liu J., McPhail L. T., McBride C. B., Steeves J. D., Ramer M. S. and Tetzlaff W. (2004) Minocycline treatment reduces delayed oligodendrocyte death, attenuates axonal dieback, and improves functional outcome after spinal cord injury. *J. Neurosci.* **24**, 2182–2190.
- Taoka Y., Okajima K., Uchiba M., Murakami K., Kushimoto S., Johno M., Naruo M., Okabe H. and Takatsuki K. (1997) Role of neutrophils in spinal cord injury in the rat. *Neuroscience* **79**, 1177–1182.
- Tian D. S., Liu J. L., Xie M. J., Zhan Y., Qu W. S., Yu Z. Y., Tang Z. P., Pan D. J. and Wang W. (2009) Tamoxifen attenuates inflammatory-mediated damage and improves functional outcome after spinal cord injury in rats. *J. Neurochem.* **109**, 1658–1667.
- Tsai L. K., Tsai M. S., Ting C. H. and Li H. (2008) Multiple therapeutic effects of valproic acid in spinal muscular atrophy model mice. *J. Mol. Med. (Berl)* **86**, 1243–1254.
- Tunnichiff G. (1999) Actions of sodium valproate on the central nervous system. *J. Physiol. Pharmacol.* **50**, 347–365.
- van der W. L., Tariq A. M., Aron B. R., Valentim L. M., Thomas D. L., Wells D. J., Latchman D. S., Gadian D. G., Lythgoe M. F. and de Belleruche J. S. (2010) Overexpression of heat shock protein 27 reduces cortical damage after cerebral ischemia. *J. Cereb. Blood Flow Metab.* **30**, 849–856.
- Vu T. H. and Werb Z. (2000) Matrix metalloproteinases: effectors of development and normal physiology. *Genes Dev.* **14**, 2123–2133.
- Wang Z., Leng Y., Tsai L. K., Leeds P. and Chuang D. M. (2011) Valproic acid attenuates blood-brain barrier disruption in a rat model of transient focal cerebral ischemia: the roles of HDAC and MMP-9 inhibition. *J. Cereb. Blood Flow Metab.* **31**, 52–57.
- Werb Z. and Chin J. R. (1998) Extracellular matrix remodeling during morphogenesis. *Ann. N. Y. Acad. Sci.* **857**, 110–118.
- Xu J., Kim G. M., Ahmed S. H., Xu J., Yan P., Xu X. M. and Hsu C. Y. (2001) Glucocorticoid receptor-mediated suppression of activator protein-1 activation and matrix metalloproteinase expression after spinal cord injury. *J. Neurosci.* **21**, 92–97.
- Yang Y., Estrada E. Y., Thompson J. F., Liu W. and Rosenberg G. A. (2007) Matrix metalloproteinase-mediated disruption of tight junction proteins in cerebral vessels is reversed by synthetic matrix metalloproteinase inhibitor in focal ischemia in rat. *J. Cereb. Blood Flow Metab.* **27**, 697–709.
- Yune T. Y., Lee J. Y., Jung G. Y., Kim S. J., Jiang M. H., Kim Y. C., Oh Y. J., Markelonis G. J. and Oh T. H. (2007) Minocycline alleviates death of oligodendrocytes by inhibiting pro-nerve growth factor production in microglia after spinal cord injury. *J. Neurosci.* **27**, 7751–7761.
- Yune T. Y., Lee J. Y., Jiang M. H., Kim D. W., Choi S. Y. and Oh T. H. (2008a) Systemic administration of PEP-1-SOD1 fusion protein improves functional recovery by inhibition of neuronal cell death after spinal cord injury. *Free Radic. Biol. Med.* **45**, 1190–1200.
- Yune T. Y., Park H. G., Lee J. Y. and Oh T. H. (2008b) Estrogen-Induced Bcl-2 Expression after Spinal Cord Injury Is Mediated through Phosphoinositide-3-Kinase/Akt-Dependent CREB Activation. *J. Neurotrauma* **25**, 1121–1131.
- Yune T. Y., Lee J. Y., Cui C. M., Kim H. C. and Oh T. H. (2009) Neuroprotective effect of *Scutellaria baicalensis* on spinal cord injury in rats. *J. Neurochem.* **110**, 1276–1287.
- Zlokovic B. V. (2005) Neurovascular mechanisms of Alzheimer's neurodegeneration. *Trends Neurosci.* **28**, 202–208.
- Zlokovic B. V. (2008) The blood-brain barrier in health and chronic neurodegenerative disorders. *Neuron* **57**, 178–201.